Institute of Paper Science and Technology
Atlanta, Georgia

IPST TECHNICAL PAPER SERIES

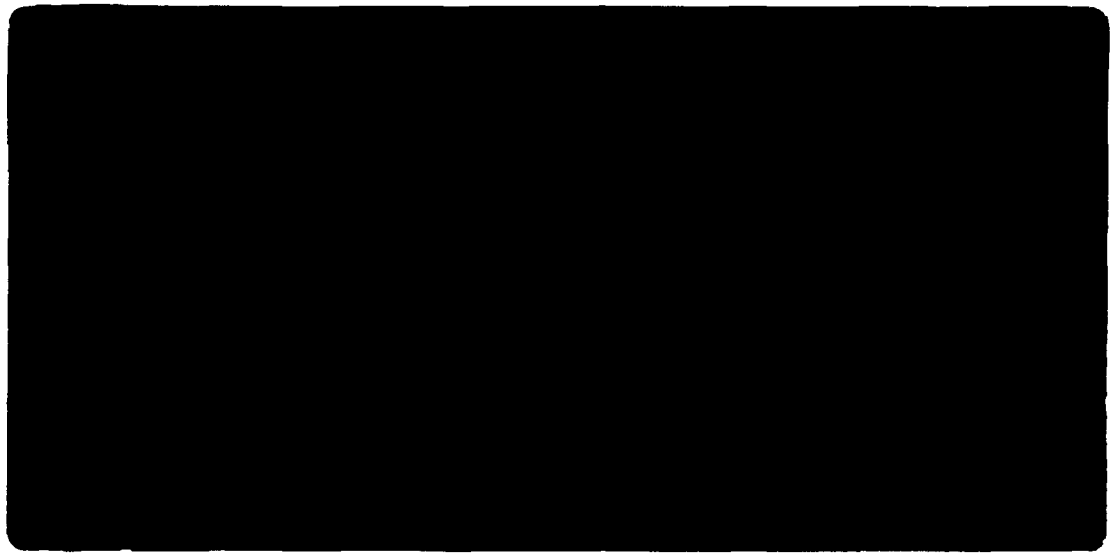

NUMBER 467

HEAT TRANSFER DURING IMPULSE DRYING: THE INFLUENCE OF PRESS IMPULSE AND PRESSURE PROFILE

D.I. ORLOFF AND P.M. PHELAN

FEBRUARY 1993

Heat Transfer During Impulse Drying: The Influence of Press Impulse and Pressure Profile

D.I. Orloff and P.M. Phelan

Submitted to
ASME National Heat Transfer Conference
August 8, 1993
Atlanta, Georgia

Table of Contents

ABSTRACT

Over the past few years, IPST has developed a ceramic-coated press roll concept that has shown promise in reducing the likelihood of sheet delamination. Limited experiments have suggested that the ceramic coating functions by decoupling heat transfer from the pressing process. In the present work, impulse drying has been simulated using a laboratory electrohydraulic press. Instantaneous heat transfer rate has been measured as a function of time during the process. Important impulse drying operating conditions such as ingoing platen surface temperature, pressure profile shape, impulse, and hydrodynamic specific surface have been systematically varied. The results of the current research indicate that for impulse drying the pressure peak should be as high as possible and shifted to the dry end of the process.

INTRODUCTION

In current practice, energy intensive evaporative drying is used to dry paper. Early research showed that a significant fraction of that energy could be saved by impulse drying (Lavery, 1988). Unfortunately, implementation of the technology was halted as impulse drying induced defects termed "sheet delamination" (Crouse, 1989).

Ongoing research at the Institute of Paper Science and Technology (IPST) has focused on process design modifications that eliminate sheet delamination. By replacing metallic press surfaces with low heat capacity, low thermal conductivity ceramics, sheet delamination can be avoided (Orloff, 1991; Orloff, 1992; Orloff and Lindsay, 1992). This paper focuses on a number of operating conditions relating to the implementation of impulse drying on a commercially configured press section.

In current practice, three presses are used to consolidate and dewater linerboard prior to evaporative drying on cylinder dryers. With the best existing technology (double-felted extended nip press), dryness at the third press rarely exceeds 48% solids in practice, but has been reported at 52% solids in pilot-scale experiments. The IPST impulse drying research team envisions installing impulse dryers after existing third presses with the objective of extending the range of pressing to about 65% solids. It may be argued that an alternate approach is to install additional double-felted extended nip presses after the third press. To assess the validity of that argument, we have recently reported pilot-scale work that shows a substantial dryness benefit and somewhat smaller strength benefit from using impulse drying (Orloff, 1992).

The objectives of the current research were to explore the interaction of impulse and pressure pulse shape on heat flux, critical temperature, and paper physical property development. As critical temperature is known to depend on the hydrodynamic specific surface of sheets to be impulse dried, the experiments were conducted with two furnishes exhibiting the extremes of specific surface to be encountered in actual practice. For

comparison purposes, double-felted pressing was also simulated for the highest impulse cases.

EXPERIMENTAL METHODS

The present work was performed using a laboratory-scale electrohydraulic press to simulate impulse drying. A ceramic-coated platen with a thin, fast, vacuum deposited copper/nickel thermocouple was mounted in the press. Temperature was recorded as a function of time during the impulse drying event and instantaneous heat flux calculated (Orloff, Jones, and Phelan, 1992).

One objective of the present research was to explore the effect of pressure pulse shape on heat flux, critical temperature, and paper physical property development. A HP3245A programmable wave generator was used to produce three different pulse shapes as shown in Figure 1.

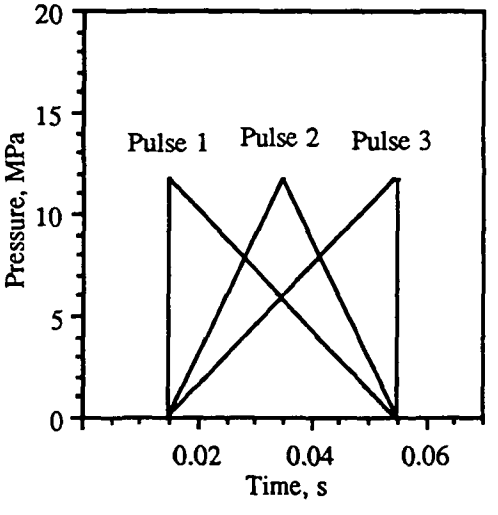

Figure 1. Wave generator output pressure profiles at an impulse of 0.23 MPa·s.

The wave generator output profiles were used to control the hydraulic servovalves on the laboratory press. Figures 2 and 3 show typical pressure profiles as recorded from the press load cell during impulse drying simulations. Limitations in the response time of the press hydraulic valves are responsible for the difference between the generator profile shapes and the recorded pressure profile shapes. For comparison, double-felted pressing simulations were also performed for pulse shapes 1 and 3 at the highest impulse. Figure 4 shows the pressure profiles used for the double-felted cases. Because the second felt has a cushioning effect, the profiles do not match the impulse drying cases exactly.

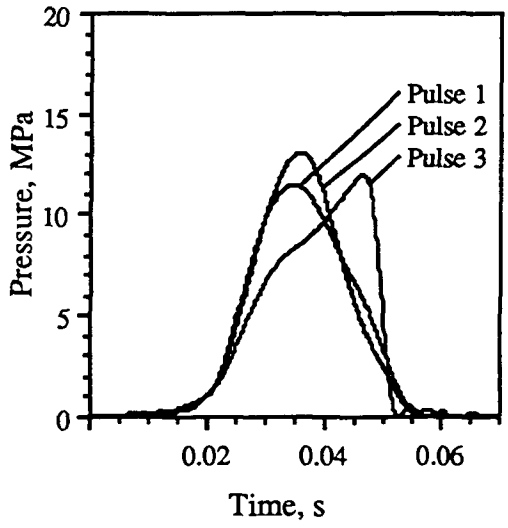

Figure 2. Impulse drying pressure profiles for different pulse shapes at an impulse of 0.23 MPa·s.

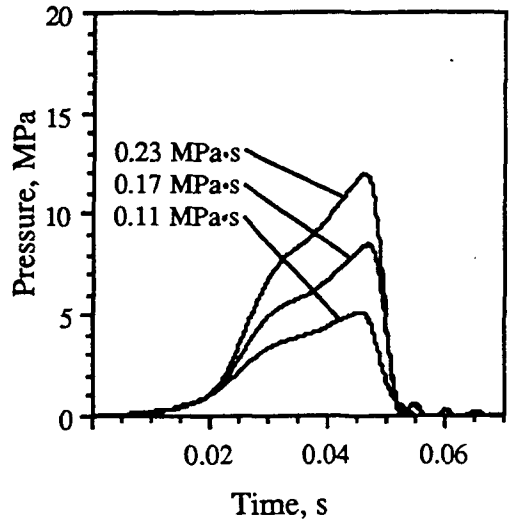

Figure 3. Pressure profiles for pulse shape 3 at different impulses.

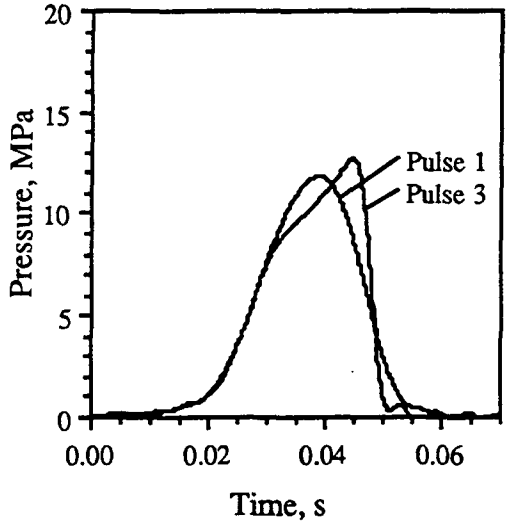

Figure 4. Double-felted drying pressure profiles at an impulse of 0.23 MPa·s.

To quantify the pressure pulse shape, a pulse shape factor was used as defined below. For the present work, the start of the impulse drying process was considered to start at a time of 0.015 s. The nip residence time was 0.04 s.

$$\text{Shape Factor} = \frac{\text{Time of Pressure Peak}}{\text{Nip Residence Time}}$$

A dynamic former was used to produce machine oriented single-ply linerboard at a basis weight of 205 g/m^2 from a high Kappa number virgin southern pine kraft (HKSP), refined to 740 ml CSF, and from recycled Southeast old corrugated containers (OCC), refined to 450 ml CSF. The hydrodynamic specific surface of these sheets, when pressed to 52% solids, was 2 m^2/g and 12 m^2/g, respectively.

After pressing to 52% solids, these sheets were preheated to 85°C and impulse dried in a laboratory-scale impulse drying simulator for 40ms at various initial platen temperatures ranging from 150°C to 400°C. Four replications were required at each initial platen temperature for physical testing. Impulse drying operating conditions were chosen to establish the relationships as stated in the objective. Table 1 shows the matrix of operating conditions that were conducted. Emphasis was placed on pulse shape 3 because earlier batch pilot-scale work had shown that doubl-felted pressing is optimized when pressure increases gradually with time in the nip (Orloff, 1992).

Table 1

Case	Furnish	Pulse Shape	Shape Factor	Impulse, MPa·s
1	HKSP	1	0.50	0.23
2		2	0.53	0.23
3L		3	0.79	0.11
3M				0.17
3H				0.23
1	OCC	1	0.50	0.23
2		2	0.53	0.23
3L		3	0.79	0.11
3M				0.17
3H				0.23
DF1	Both	1	0.60	0.23
DF3	Both	3	0.75	0.23

DISCUSSION OF RESULTS

Heat Flux and Energy Transfer

Early work has suggested that heat flux and energy transfer during impulse drying is not sensitive to impulse as long as the thermal properties of the impulse drying surface are sufficiently low (Orloff, 1992). In the present work, the authors were looking for subtle changes in the shape of the heat flux curve with changes in impulse and pressure pulse shape. Figures 5 through 8 show energy transfer to the sheet during impulse drying as a function of initial platen surface temperature for the two furnishes at varying impulse and pulse shape. The figures show that energy transfer increases with increasing initial platen temperature, increasing impulse, and increasing hydrodynamic specific surface. Energy transfer was not found to depend on pressure pulse shape.

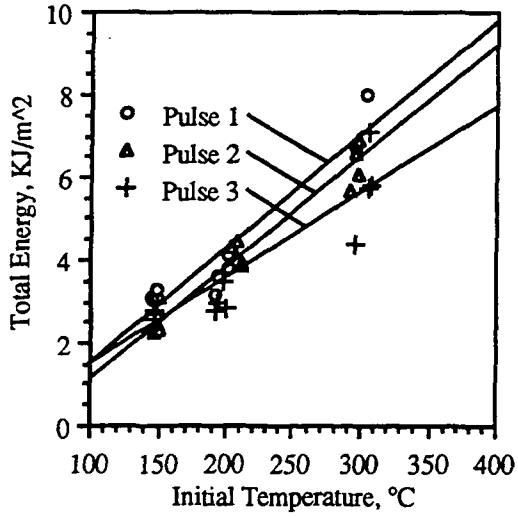

Figure 5. Energy transferred for an impulse of 0.23 MPa·s and the HKSP low specific surface furnish.

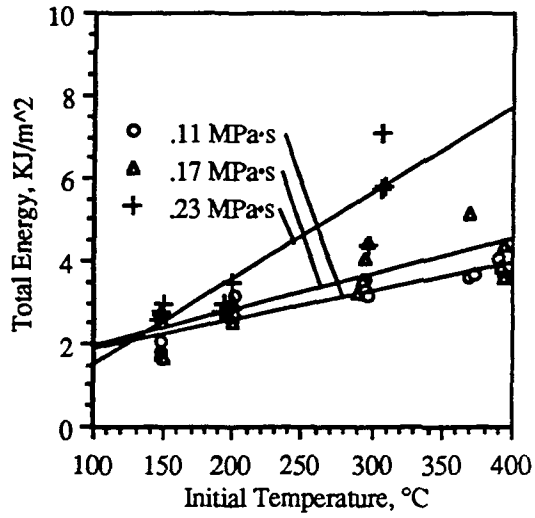

Figure 6. Energy transferred for pulse shape 3 and the HKSP low specific surface furnish.

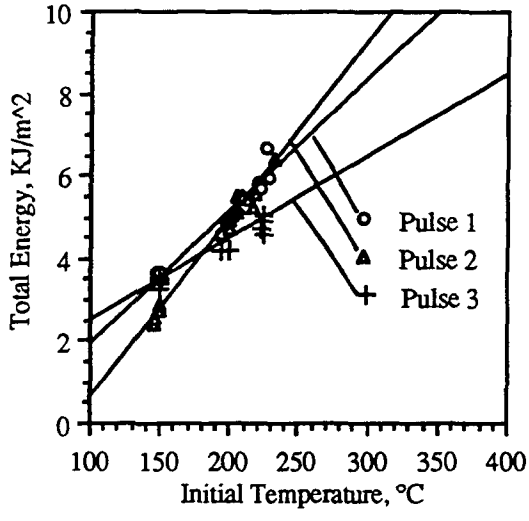

Figure 7. Energy transferred for an impulse of 0.23 MPa·s and the OCC high specific surface furnish.

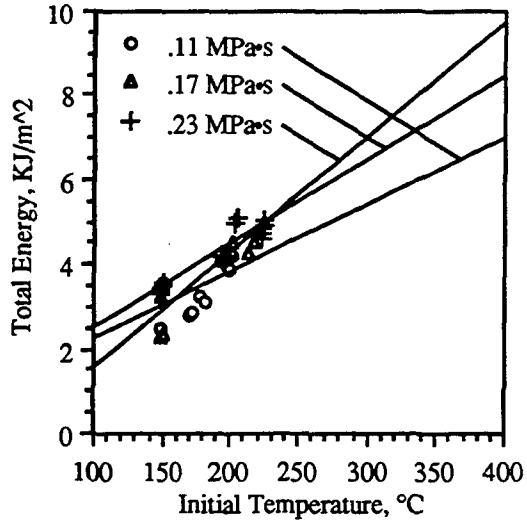

Figure 8. Energy transferred for pulse shape 3 and the OCC high specific surface furnish.

For the low specific surface HKSP furnish, energy transfer is independent of pulse shape but increases for increasing impulse (pressure). Energy transfer for the high specific surface OCC furnish is independent of impulse (pressure) consistent with previous work (Orloff, 1992). For these sheets, there was slightly higher energy transfer for pulse shapes 1 and 2.

In order to observe differences in the shape of the heat flux curve, certain landmarks on the curve were defined. Figures 9 and 10 show typical heat flux curves for pulse shapes 1 and 3 near the critical temperature (defined in the next section) for each furnish. Indicated are the heat flux first and second peaks.

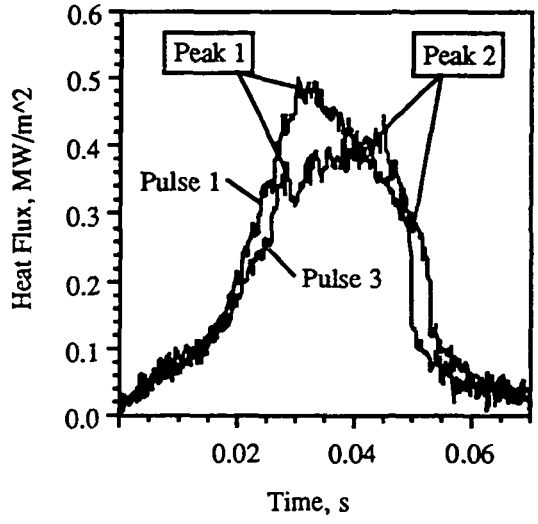

Figure 9. Heat flux for HKSP furnish at an impulse of 0.23 MPa·s and an initial temperature of 300°C.

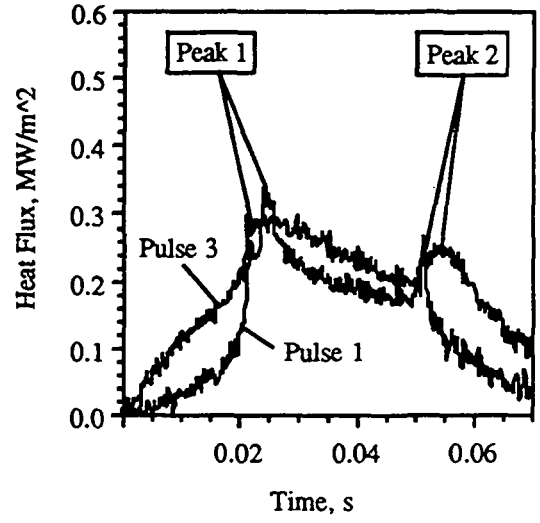

Figure 10. Heat flux for OCC furnish at an impulse of 0.23 MPa·s and an initial temperature of 200°C.

Of interest are the magnitude of these heat flux peaks and the time at which they occur in the impulse drying process. Figures 11 and 12 show the first and second peak heat flux as a function of initial platen surface temperature for the low specific surface furnish for the various pulse shapes. Shifting the peak pressure to the dry end of the nip results in a decrease in the rate of growth of the first peak and an increased growth rate of the second peak heat flux with platen temperature. This suggests that the rate of heat transfer is controlled by the shape of the pressure pulse.

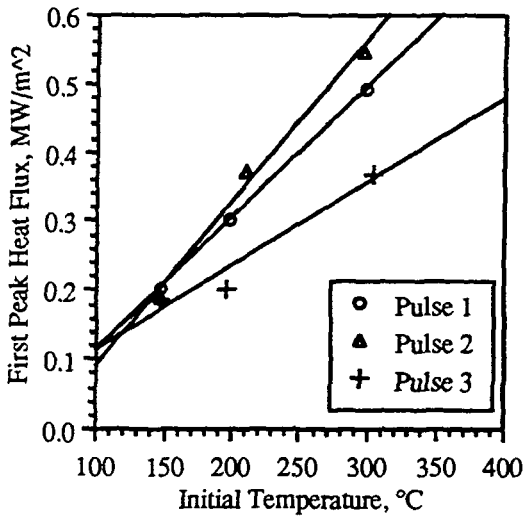

Figure 11. First heat flux peak for an impulse of 0.23 MPa·s and the HKSP low specific surface furnish.

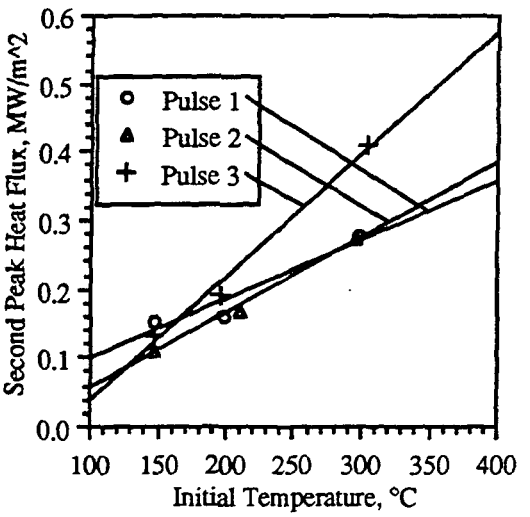

Figure 12. Second heat flux peak for an impulse of 0.23 MPa·s and the HKSP low specific surface furnish.

A similar analysis may be performed on the sheets made from recycled pulp as shown in Figures 13 and 14. It is of interest to note that for this furnish the rate of change for the heat flux peaks does not change when the peak pressure is shifted to the dry end of the nip.

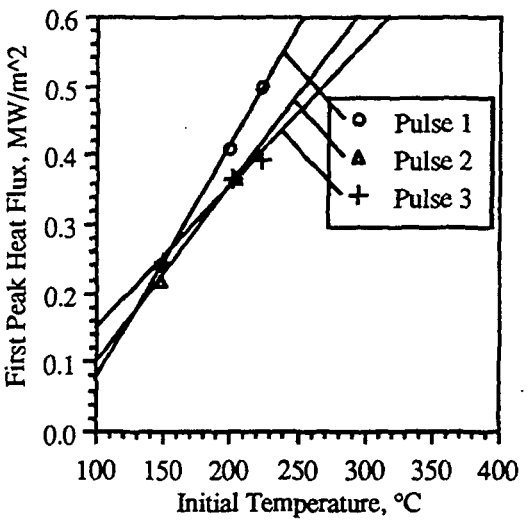

Figure 13. First heat flux peak for an impulse of 0.23 MPa·s and the OCC high specific surface furnish.

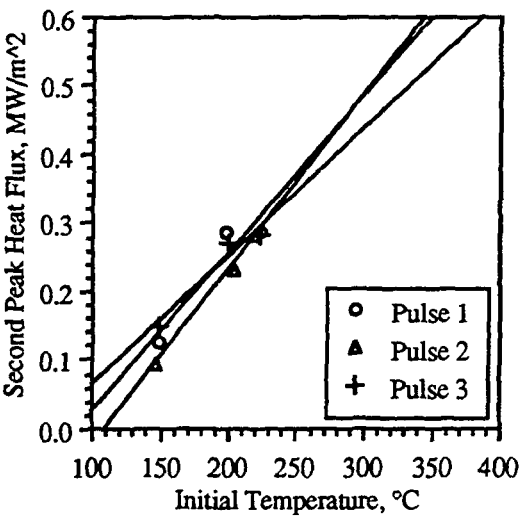

Figure 14. Second heat flux peak for an impulse of 0.23 MPa·s and the OCC high specific surface furnish.

For the low specific surface HKSP furnish, shifting the peak pressure to the dry end of the process results in decreasing the time at which the second heat flux peak occurs as shown in Figure 15. Also, for all pulse shapes, the first heat flux peak occurs later at higher

temperatures. Increasing the specific surface of the sheet (OCC furnish) results in an earlier first heat flux peak as shown in Figure 16. For this furnish, the second peak occurs earlier than the HKSP furnish peaks at higher temperatures.

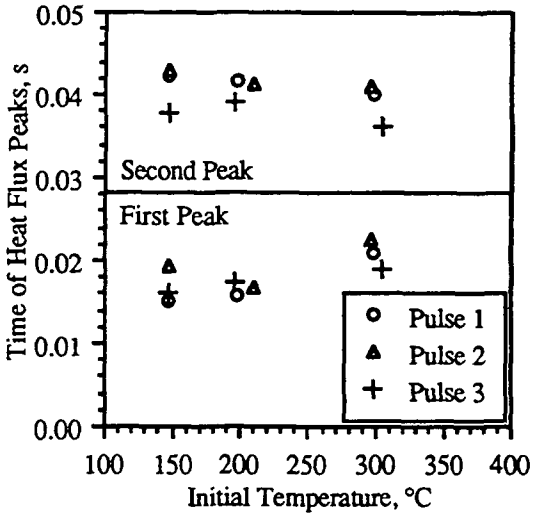

Figure 15. Time of heat flux peaks for an impulse of 0.23 MPa·s and the HKSP low specific surface furnish.

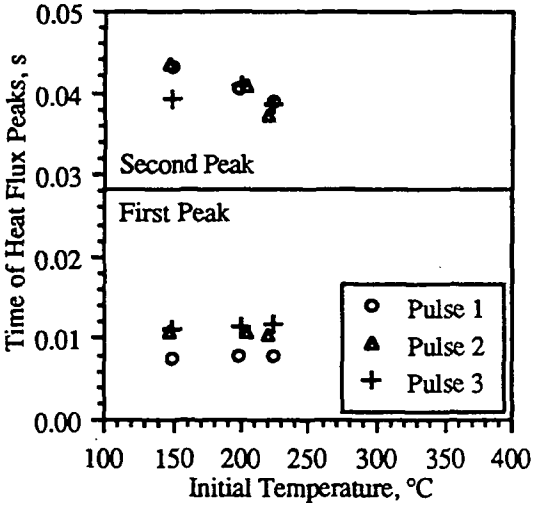

Figure 16. Time of heat flux peaks for an impulse of 0.23 MPa·s and the OCC high specific surface furnish.

The shape of the heat flux curve is dependent on the shape of the pressure curve only for low hydrodynamic specific surface furnishes. Heat flux peaks are higher, and the first peak occurs sooner for high hydrodynamic specific surface furnishes. This indicates that energy transfer occurs earlier for dense, closed sheets.

In Figures 17 through 22, similar plots were generated to determine the influence of impulse for pressure profile shape 3. It is observed that the rate of change for the first and second peak heat fluxes increases with increased impulse for the low specific surface furnish. The rate of change increases with an increase in specific surface, but for the high specific surface furnish the rate of change is independent of impulse. Also, observe that increasing the impulse decreases the times at which the peak heat fluxes are observed.

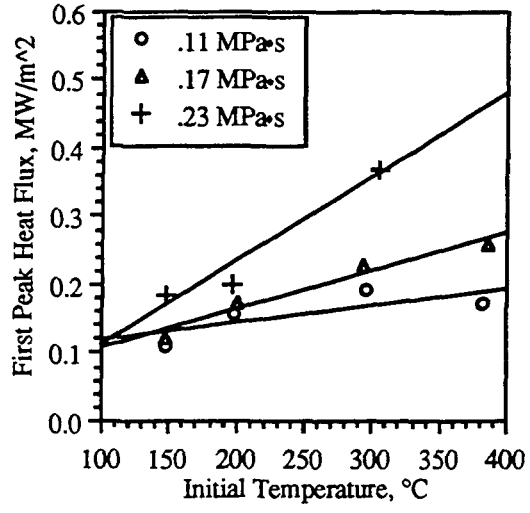

Figure 17. First heat flux peak for pulse shape 3 and the HKSP low specific surface furnish.

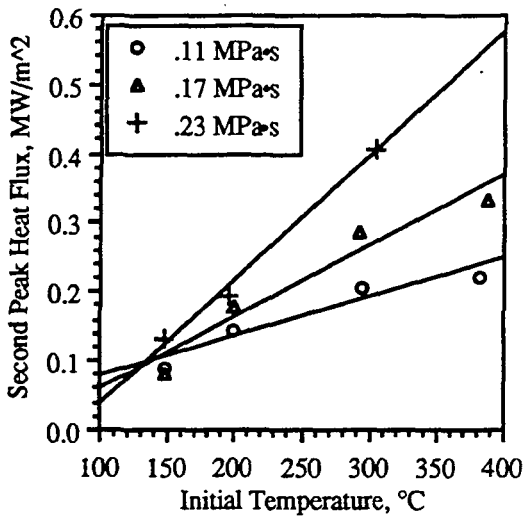

Figure 18. Second heat flux peak for pulse shape 3 and the HKSP low specific surface furnish.

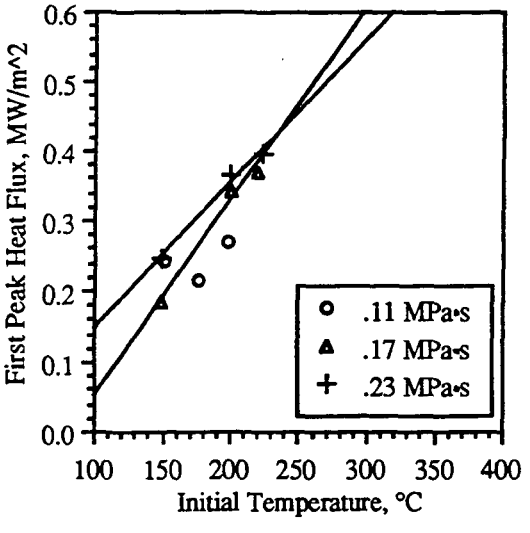

Figure 19. First heat flux peak for pulse shape 3 and the OCC high specific surface furnish.

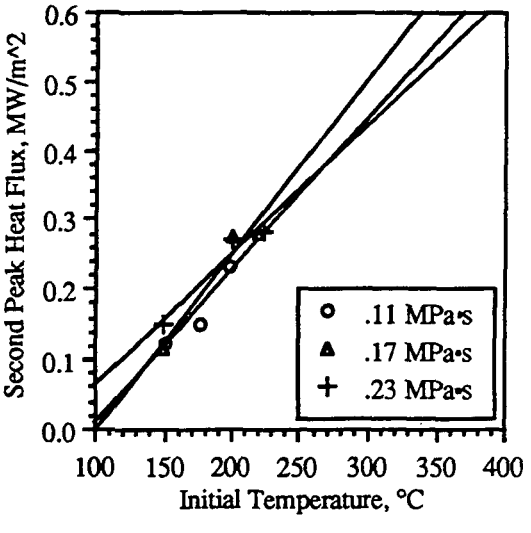

Figure 20. Second heat flux peak for pulse shape 3 and the OCC high specific surface furnish.

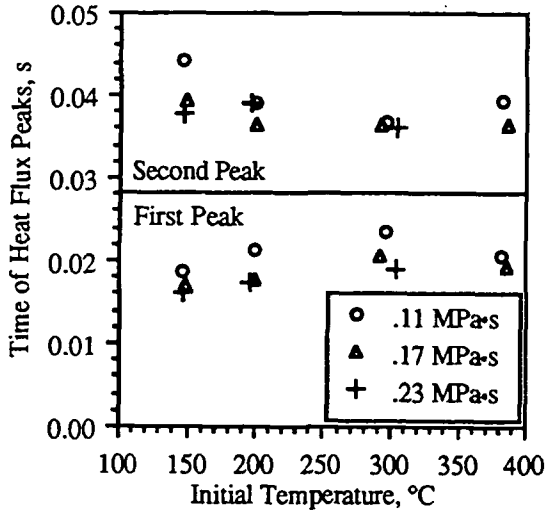

Figure 21. Time of heat flux peaks for pulse shape 3 and the HKSP low specific surface furnish.

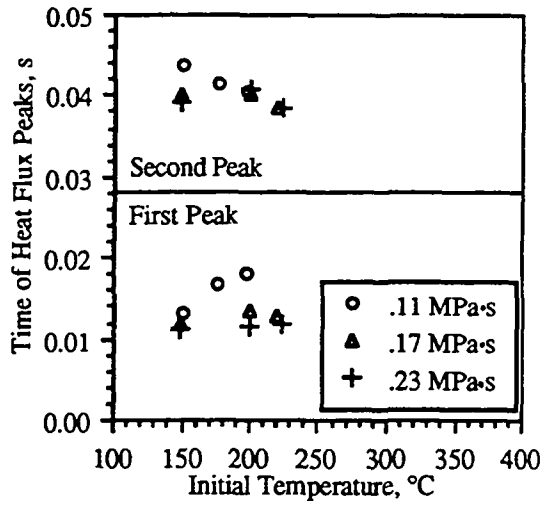

Figure 22. Time of heat flux peaks for pulse shape 3 and the OCC high specific surface furnish.

Earlier laboratory work has suggested that energy transfer for a furnish with a hydrodynamic specific surface of 4-5 m^2/g was independent of pressure at impulses ranging from 0.06 to 0.13 MPa·s (Orloff, 1992). The data presented in this paper are consistent with the previous results in the same range of impulse.

In summary, for low hydrodynamic specific surface furnishes, peak pressure influences energy transfer at impulses greater than 0.17 MPa·s, and the heat flux peak occurs near the pressure peak. For high hydrodynamic specific surface furnishes, energy transfer occurs early in the impulse drying process, but is independent of peak pressure and pressure profile shape.

Critical Temperatures

A major objective of these experiments was to determine the effect of pressure pulse shape and impulse on critical impulse drying temperature, defined as the highest initial platen surface temperature that does not result in sheet delamination. As in previous work, sheet delamination was determined by out-of-plane ultrasonic testing. In Appendix A, Figures A1-A20 show the specific elastic modulus and the coefficient of variation of the specific elastic modulus used to determine the critical temperatures.

Figure 23 shows the effect of impulse on critical temperature for pressure pulse shape 3. The critical temperature increases with increased impulse for the HKSP low specific surface furnish and decreases with increased impulse for the OCC high specific surface furnish. The effect of pulse shape on critical temperature at a given impulse is shown in Figure 24. It is observed that critical temperature increases when the peak pressure is shifted to the dryer side of the nip.

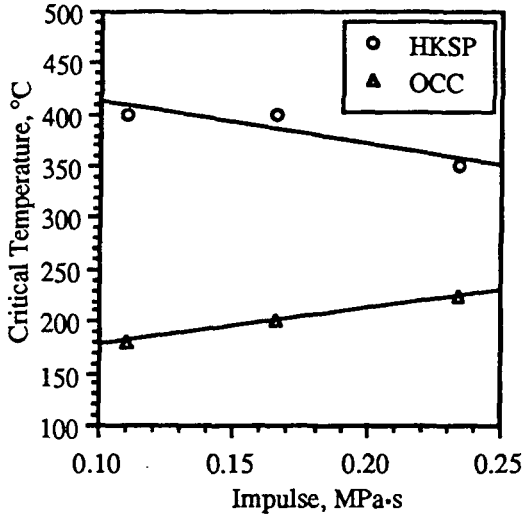

Figure 23. Critical temperatures for pressure pulse shape 3 at different impulses.

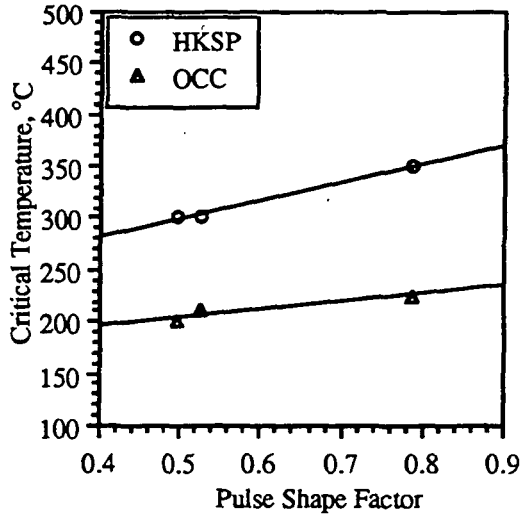

Figure 24. Critical temperatures for different pressure pulses and an impulse of 0.23 MPa·s.

As shown in Figure 25, the energy transfer at the critical temperature is independent of specific surface and pulse shape. This indicates that the onset of delamination is a function of total energy transferred at a given impulse (peak pressure). Confirming the data in previous work (Orloff and Sobczynski, 1992), Figure 26 shows critical temperature decreasing with increased specific surface.

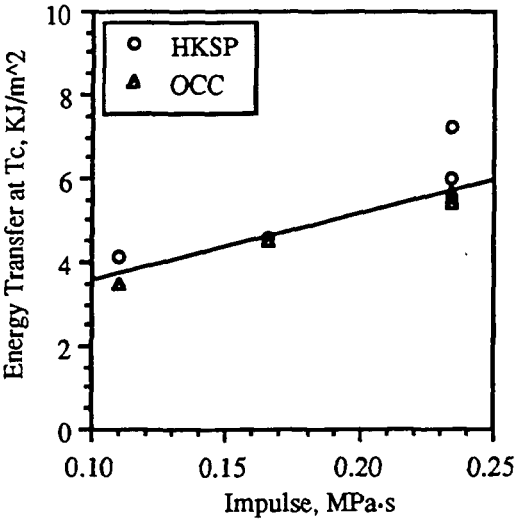

Figure 25. Energy transfer at critical temperature for all cases.

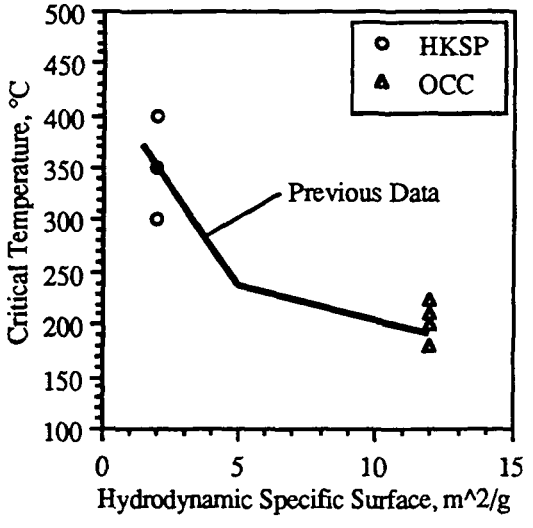

Figure 26. Critical temperature for all cases compared to the best fit of data from previous work (Orloff and Sobczynski, 1992).

In summary, the critical impulse drying temperature is a function of hydrodynamic specific surface, pressure pulse shape, and impulse (peak pressure). Although heat flux is also a function of the same variables, total energy transfer at the critical temperature is only a function of impulse.

Water Removal and Paper Physical Properties

The ultimate objective of impulse drying is to increase water removal and improve paper physical properties. For these experiments, moisture ratio change and cross direction STFI compression index at respective critical temperatures are shown in Figures 27 through 30. For the low specific surface furnish, Figures 27 and 28 show that increased impulse will result in higher strength without improving dryness, but water removal is better than double-felted pressing. For the high specific surface furnish, Figures 27 and 28 show that increased impulse will improve dryness but will not improve strength. As expected, water removal decreases with increased specific surface.

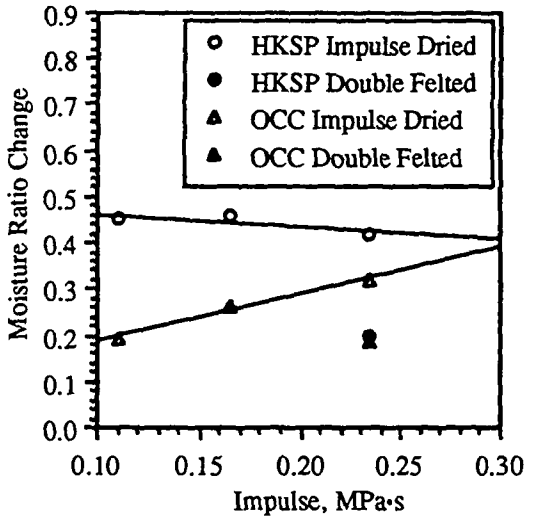

Figure 27. Moisture ratio change for pulse shape 3 compared to double-felted pressing.

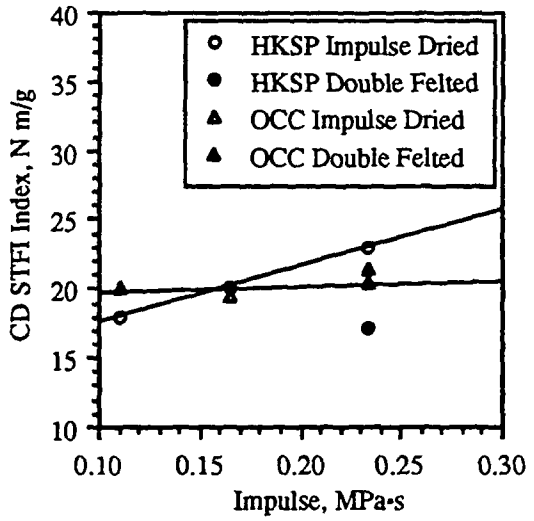

Figure 28. CD STFI Index for pulse shape 3 compared to double-felted pressing.

The effect of pressure pulse shape on water removal and CD STFI index is shown in Figures 29 and 30. It is observed that shifting the peak pressure to the dryer side of the nip results in a small improvement in water removal but no improvement in compression strength. In terms of water removal, impulse drying was superior to double-felted pressing. In terms of cross direction compression index, impulse drying gave superior strength for the low specific surface virgin furnish while showing comparable strength for the recycled high specific surface furnish.

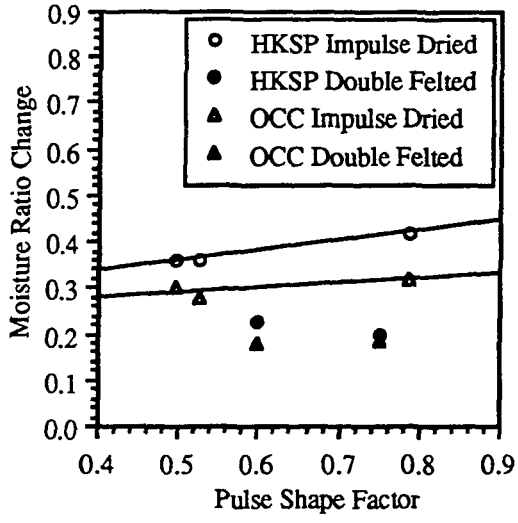

Figure 29. Moisture ratio change for impulse of 0.23 MPa·s compared to double-felted pressing.

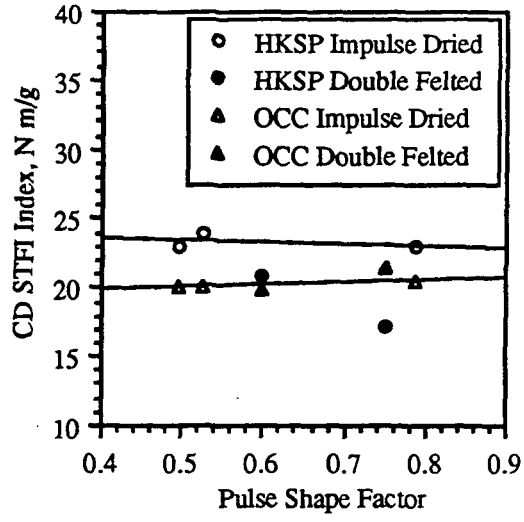

Figure 30. CD STFI index for impulse of 0.23 MPa·s compared to double-felted pressing.

Water removal is a function of critical temperature as shown in Figure 31. It is observed that for impulse drying, water removal is independent of furnish, pressure pulse shape, and impulse for the range of 0.11 to 0.23 MPa·s.

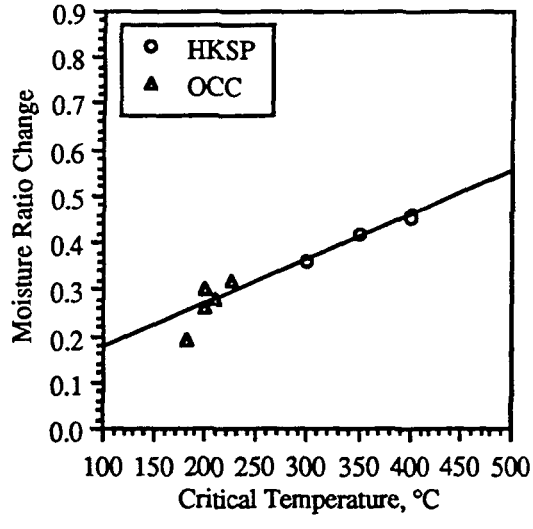

Figure 31. Moisture ratio change for all cases at critical temperature.

Table 2 summarizes the water removal and CD STFI index at the critical temperature for all cases tested. Also, the outgoing solids, IPC density, MD STFI index, and the z-direction specific elastic modulus are tabulated at the critical temperatures. All the water removal and sheet physical property data are shown in the Appendices. In summary, impulse drying

improves water removal over double-felted pressing for all cases investigated. Paper physical properties are improved over double-felted pressing or are comparable.

Table 2

Case	Critical Temp. ℃	Moisture Ratio Change	Outgoing Solids %	IPC Density kg/m^3	CD STFI Index N m/g	MD STFI Index N m/g	Specific Elastic Modulus MN m/kg
HKSP 1	300	.36	66	760	23	39	.25
HKSP 2	300	.36	67	755	24	38	.22
HKSP 3L	400+	.45	64	650	18	29	.10
HKSP 3M	400+	.46	67	730	20	32	.19
HKSP 3H	350	.42	67	770	23	34	.24
HKSP DF1	n/a	.23	58	632	21	30	.12
HKSP DF3	n/a	.20	60	663	17	27	.16
OCC 1	200	.30	63	765	20	32	.23
OCC 2	210	.28	63	755	20	32	.24
OCC 3L	180	.19	60	720	20	31	.21
OCC 3M	200	.26	63	745	20	32	.21
OCC 3H	225	.32	65	780	20	32	.26
OCC DF1	n/a	.18	61	725	20	31	.24
OCC DF3	n/a	.18	63	731	21	26	.24

CONCLUSIONS

Heat flux is dependent on hydrodynamic specific surface. For low specific surface furnishes, heat flux correlates to the pressure pulse shape and peak pressure. Heat flux for furnishes with a higher specific surface will be greater in the early portion of the impulse drying process but will be independent of other process variables.

Total energy transfer is pressure dependent only for low specific surface furnishes and pressure pulse shape dependent only for high specific surface furnishes. However, at the impulse drying critical temperatures, total energy transfer is only a function of impulse.

Impulse drying critical temperature as determined by sheet delamination is a function of pressure pulse shape, impulse, and hydrodynamic specific surface. Shifting the pressure peak to the dry end of the process increases the critical temperature. For high specific surfaces, increasing impulse increases the critical temperature.

Increased critical temperature increases water removal. Water removal for impulse drying is superior to double-felted pressing for all conditions investigated. Paper strength development for impulse drying is comparable or superior to double-felted pressing and appears to be primarily a function of furnish and impulse.

The objective of the current research was to explore the interaction of impulse and pressure pulse shape on heat flux, critical temperature, and paper physical property development. This data will be used to determine optimal operating conditions for demonstrating impulse drying on a commercial scale. The results of the current research indicate that for impulse drying the pressure peak should be as high as possible and shifted to the dry end of the process.

RECOMMENDATIONS FOR FUTURE WORK

Pressure pulse shape is an important variable in impulse drying. Further fundamental work should be undertaken to determine the optimal pressure pulse shape for a commercial impulse dryer. This will require modifications to the electrohydraulic press which are planned for the second quarter of 1993.

In the present work, the peak pressure was changed to vary the impulse. Some of the effects observed may be a function of peak pressure independent of nip residence time. When the modifications to the electrohydraulic press are completed, further experiments should be undertaken to separate the effect of peak pressure from nip residence time.

New platen surfaces with higher "thermal mass" may reduce sheet sticking and increase roll long-term durability. The influence of pressure pulse shape and impulse on impulse drying performance needs to be investigated for these surfaces. This work will be undertaken as a student project in 1993.

ACKNOWLEDGEMENTS

The work reported was supported by the member companies of the Institute of Paper Science and Technology and by the U.S. Department of Energy Office of Industrial Programs through Grant No. DE-FGO2-85CE40738. Their support is gratefully acknowledged. The authors would like to thank I. Rudman for coordinating and performing the physical testing. M. Abazeri and the personnel of the IPST Research Services Division were very helpful in performing the required testing and are gratefully acknowledged.

REFERENCES

Batakis, A.P., and Vogan, J.W., 1985, "Rocket Thrust Chamber Thermal Barrier Coatings," NASA CR-175022.

Crouse, J.W., Woo, Y.D., and Sprague, C.H., 1989, "Delamination-A Stumbling Block To Implementing Impulse Drying Technology For Linerboard," *Tappi Journal*, pp. 211-215.

Giedt, W.H., 1955, "The Determination of Transient Temperatures and Heat Transfer at a Gas-Metal Interface Applied to a 40-mm Gun Barrel," *Jet Propulsion*, Vol. 25, pp. 158-162.

Lavery, H.P., 1988, "High-Intensity Drying Processes-Impulse Drying," Report 3, DOE/CE/40738-T3.

Nanigian, J., "Rocket Igniter Characteristics," Reprinted from Instruments & Control Systems in NANMAC *Temperature Handbook*, Vol. 7, pp. L7-L10.

Orloff, D.I., 1992, "Impulse Drying of Linerboard: Control of Delamination," Presented at the 77th Annual Meeting of the Canadian Pulp and Paper Association, to be published in *Journal of Pulp and Paper Science*.

Orloff, D.I., 1991, "Impulse Drying: Controlling Delamination in Heavy Weight Grades," *Institute of Paper Science and Technology Executives' Conference Proceedings*, pp. 24-27.

Orloff, D.I., 1991, "High-Intensity Drying Processes-Impulse Drying," Report 6, DOE/CE/40738-T6.

Orloff, D.I., 1992, "A Comparision of Impulse Drying to Double Felted Pressing on Pilot-Scale Shoe Presses and Roll Presses," Report 7, DOE/CE/40738-T7.

Orloff, D.I., and Lindsay, J.D., 1992, "The Influence of Yield, Refining and Ingoing Solids on the Impulse Drying Performance of a Ceramic Coated Press Roll," to be presented at the 1992 TAPPI Papermakers Conference.

Orloff, D.I., Jones, G.L., Phelan, P.M., 1992, "The Effects of Heating Mode on Roll Durability and Efficiency of Impulse Drying," *ASME Fundamentals of Heat Transfer in Porous Media*, pp. 141-150.

Orloff, D.I., 1992, "Impulse Drying of Paper: A Review of Recent Research," *Industrial Energy Technology Conference Proceedings*, pp. 110-116.

Orloff, D.I., and Sobczynski, S.F., 1992, "Impulse Drying Pilot Press Demonstration: Ceramic Surfaces Inhibit Delamination," *The European Pulp and Paper Week 4th International Conference Proceedings*, pp. 180-198.

Signed: 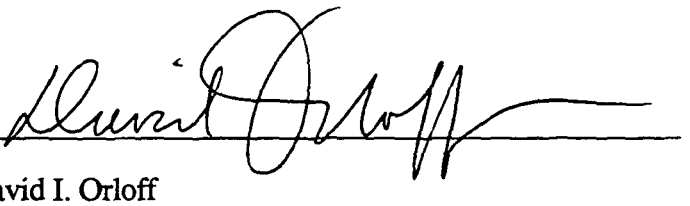

David I. Orloff
Professor of Engineering
Acting Director Engineering & Paper Materials Division

Signed: 

Paul M. Phelan
Assistant Scientist

APPENDIX A

Specific elastic modulus and coefficient of variation of the specific elastic modulus for each impulse drying case used to determine the onset of sheet delamination.

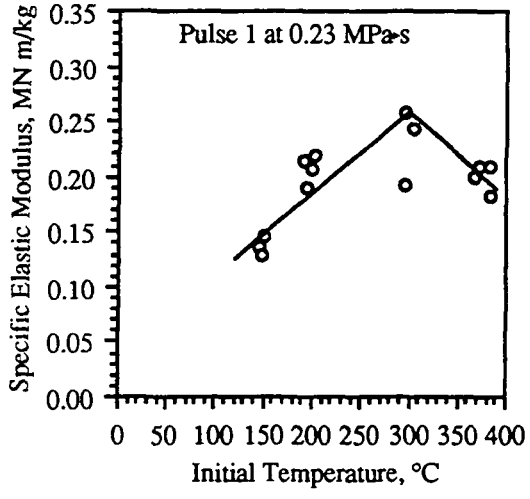

Figure A1. Specific elastic modulus for the HKSP furnish with pulse shape 1 at 0.23 MPa·s.

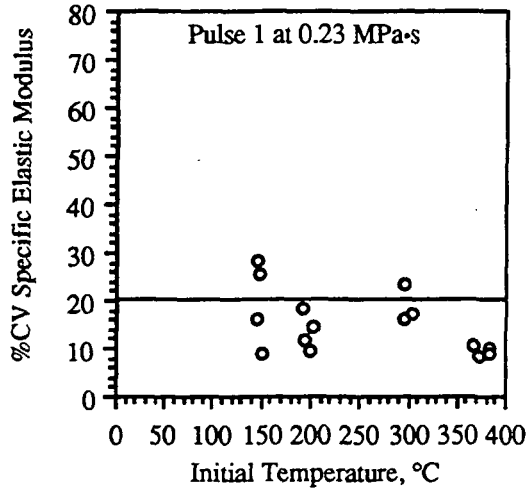

Figure A2. Coefficient of variation of the specific elastic modulus for the HKSP furnish with pulse shape 1 at 0.23 MPa·s.

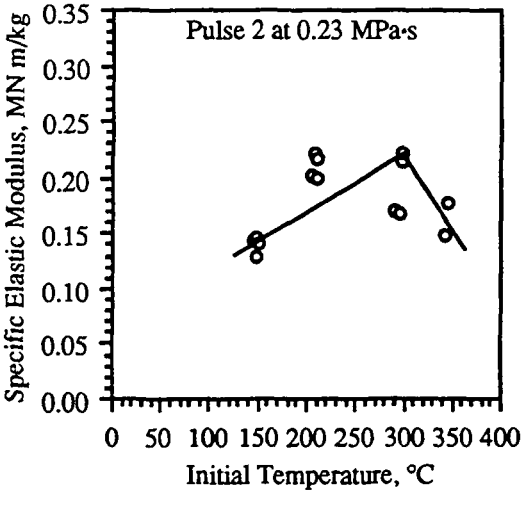

Figure A3. Specific elastic modulus for the HKSP furnish with pulse shape 2 at 0.23 MPa·s.

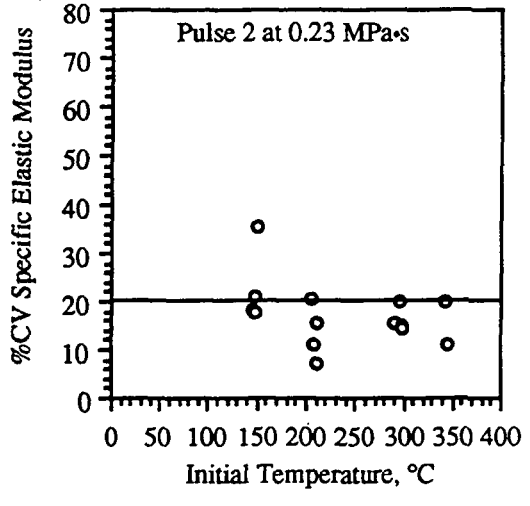

Figure A4. Coefficient of variation of the specific elastic modulus for the HKSP furnish with pulse shape 2 at 0.23 MPa·s.

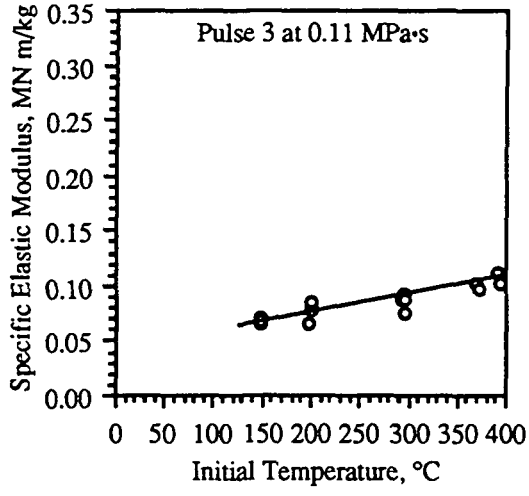

Figure A5. Specific elastic modulus for the HKSP furnish with pulse shape 3 at 0.11 MPa·s.

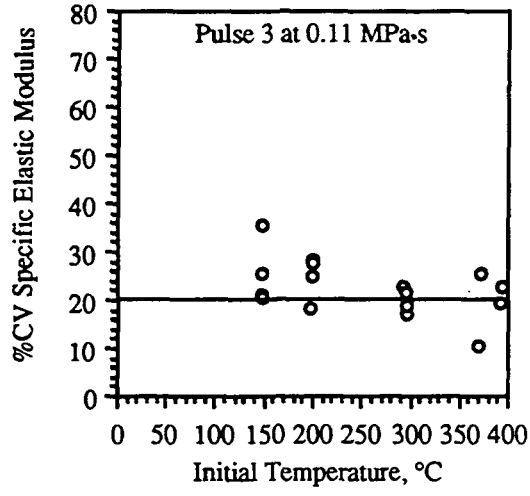

Figure A6. Coefficient of variation of the specific elastic modulus for the HKSP furnish with pulse shape 3 at 0.11 MPa·s.

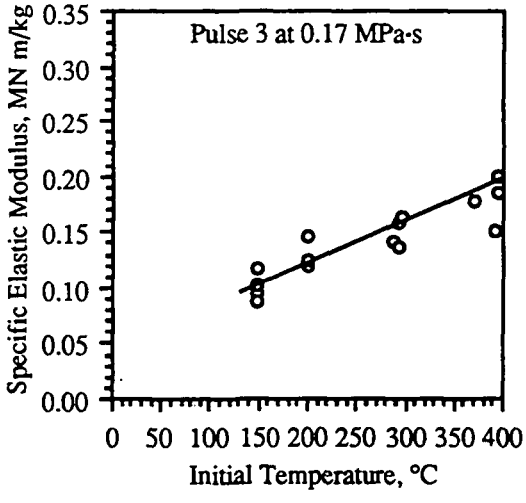

Figure A7. Specific elastic modulus for the HKSP furnish with pulse shape 3 at 0.17 MPa·s.

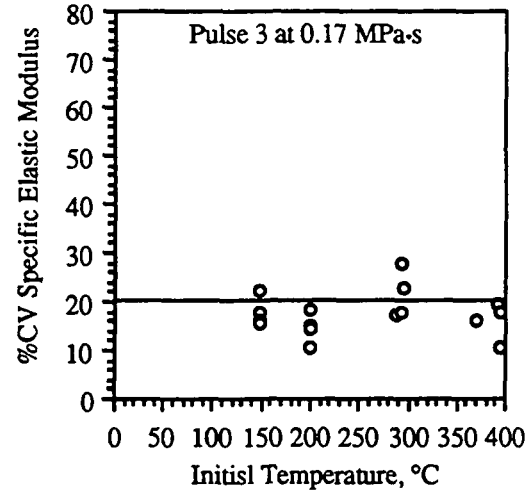

Figure A8. Coefficient of variation of the specific elastic modulus for the HKSP furnish with pulse shape 3 at 0.17 MPa·s.

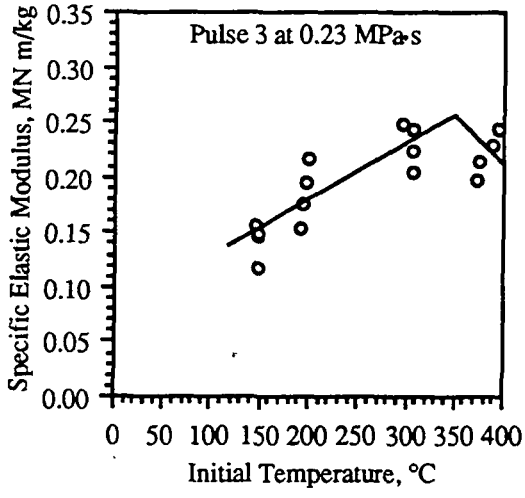

Figure A9. Specific elastic modulus for the HKSP furnish with pulse shape 3 at 0.23 MPa·s.

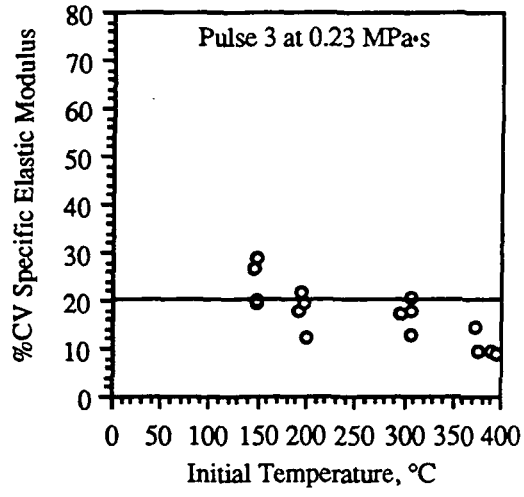

Figure A10. Coefficient of variation of the specific elastic modulus for the HKSP furnish with pulse shape 3 at 0.23 MPa·s.

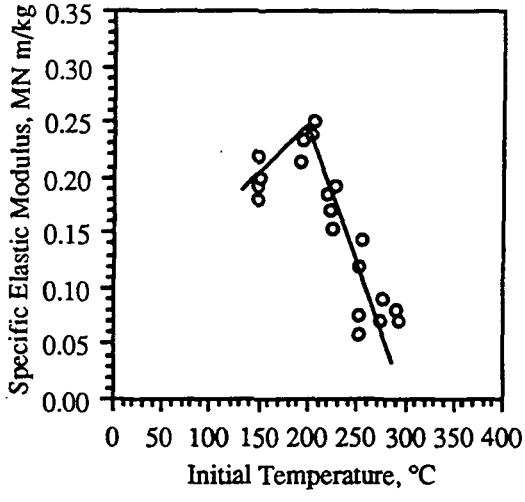

Figure A11. Specific elastic modulus for the OCC furnish with pulse shape 1 at 0.23 MPa·s.

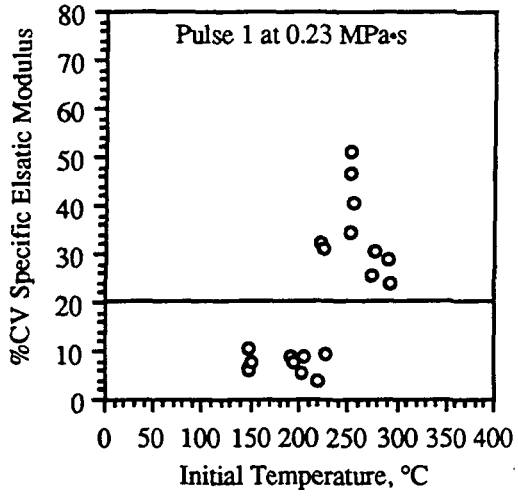

Figure A12. Coefficient of variation of the specific elastic modulus for the OCC furnish with pulse shape 1 at 0.23 MPa·s.

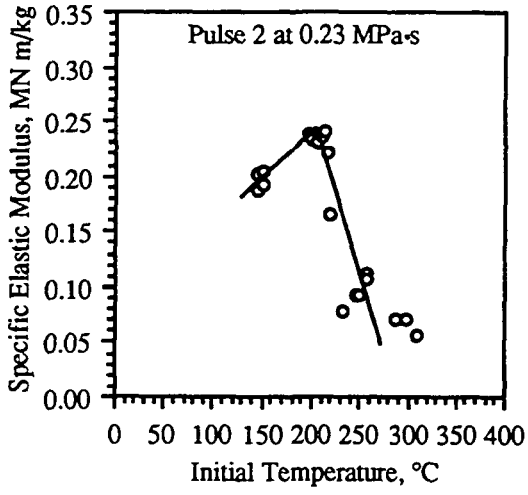

Figure A13. Specific elastic modulus for the OCC furnish with pulse shape 2 at 0.23 MPa·s.

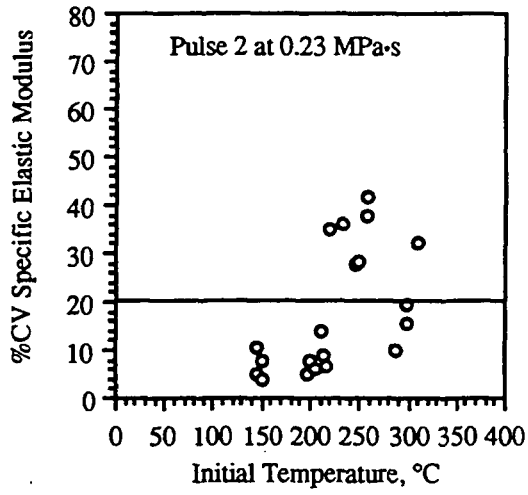

Figure A14. Coefficient of variation of the specific elastic modulus for the OCC furnish with pulse shape 2 at 0.23 MPa·s.

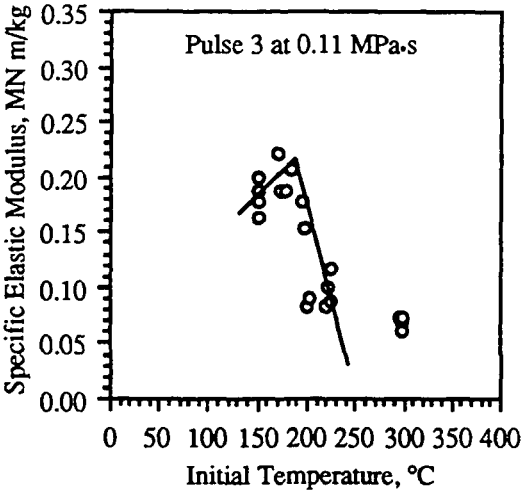

Figure A15. Specific elastic modulus for the OCC furnish with pulse shape 3 at 0.11 MPa·s.

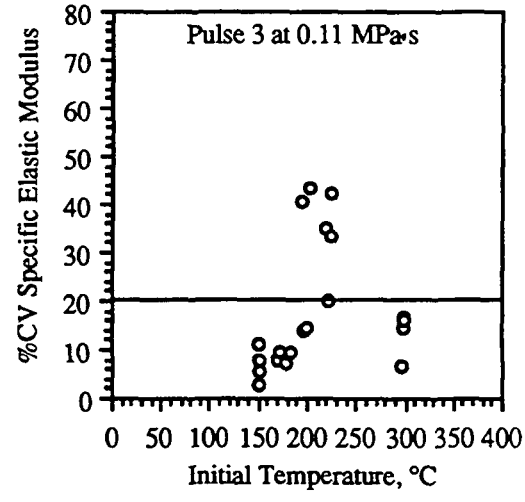

Figure A16. Coefficient of variation of the specific elastic modulus for the OCC furnish with pulse shape 3 at 0.11 MPa·s.

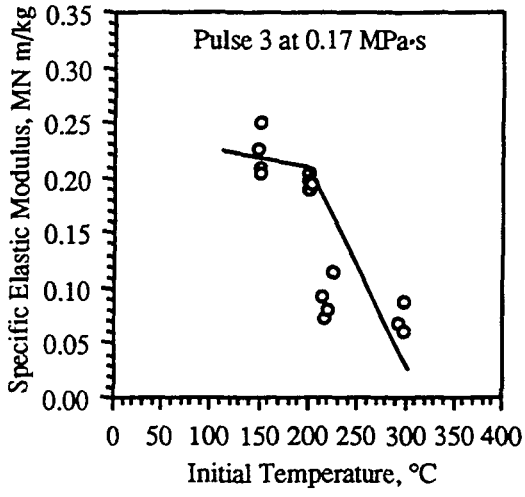

Figure A17. Specific elastic modulus for the OCC furnish with pulse shape 3 at 0.17 MPa·s.

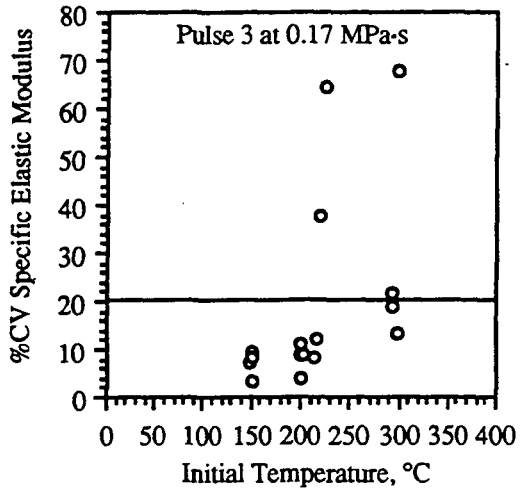

Figure A18. Coefficient of variation of the specific elastic modulus for the OCC furnish with pulse shape 3 at 0.17 MPa·s.

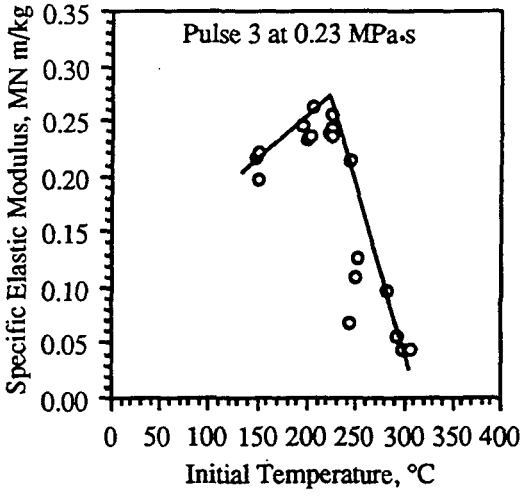

Figure A19. Specific elastic modulus for the OCC furnish with pulse shape 3 at 0.23 MPa·s.

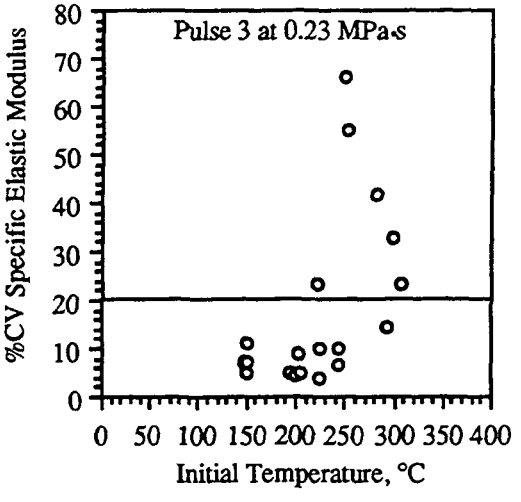

Figure A20. Coefficient of variation of the specific elastic modulus for the OCC furnish with pulse shape 3 at 0.23 MPa·s.

APPENDIX B

Figures B1-B10 show the moisture ratio change for each impulse drying case. Data for delaminated samples are not shown.

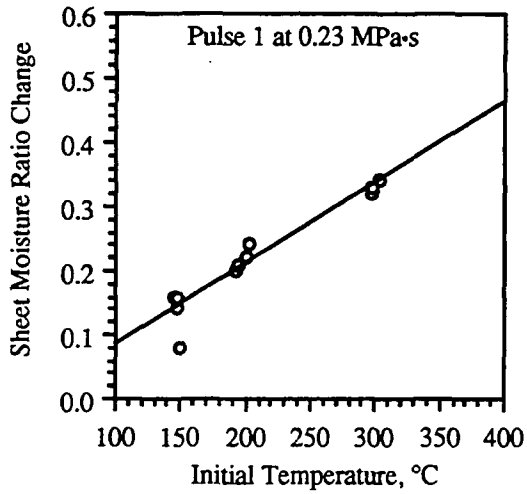

Figure B1. Moisture ratio change for the HKSP furnish with pulse shape 1 at 0.23 MPa·s.

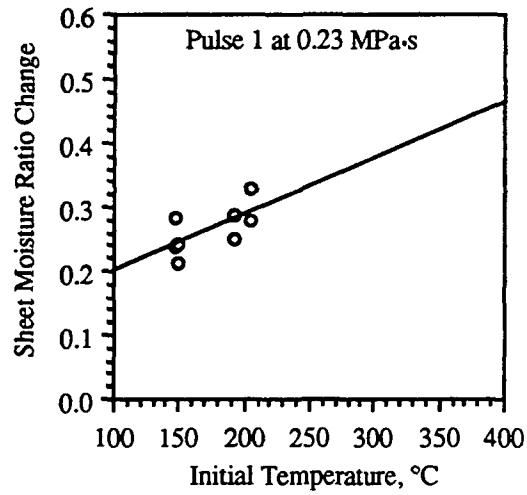

Figure B2. Moisture ratio change for the OCC furnish with pulse shape 1 at 0.23 MPa·s.

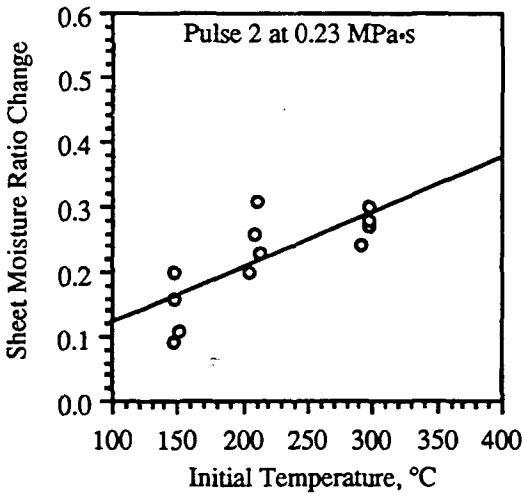

Figure B3. Moisture ratio change for the HKSP furnish with pulse shape 2 at 0.23 MPa·s.

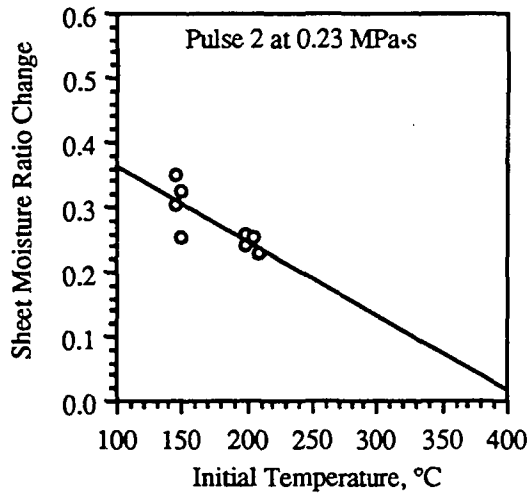

Figure B4. Moisture ratio change for the OCC furnish with pulse shape 2 at 0.23 MPa·s.

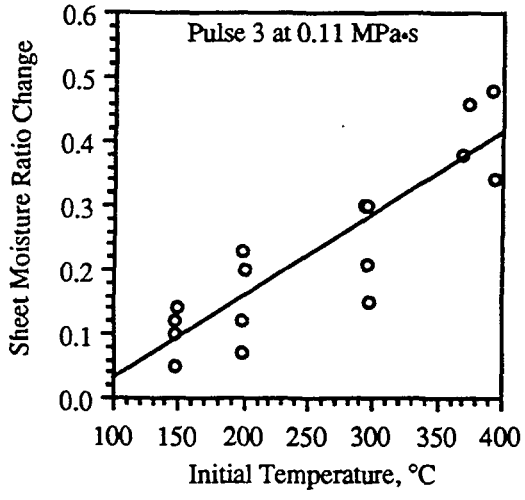

Figure B5. Moisture ratio change for the HKSP furnish with pulse shape 3 at 0.11 MPa·s.

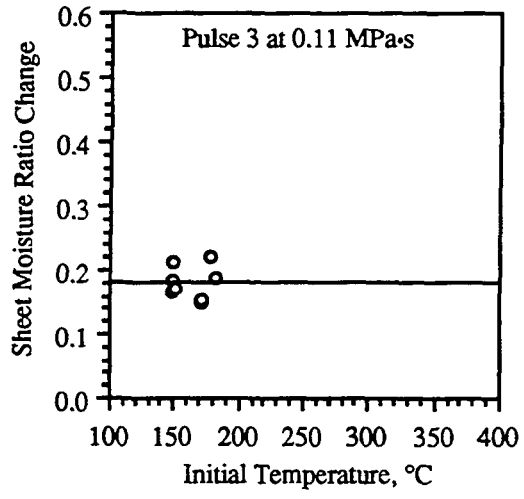

Figure B6. Moisture ratio change for the OCC furnish with pulse shape 3 at 0.11 MPa·s.

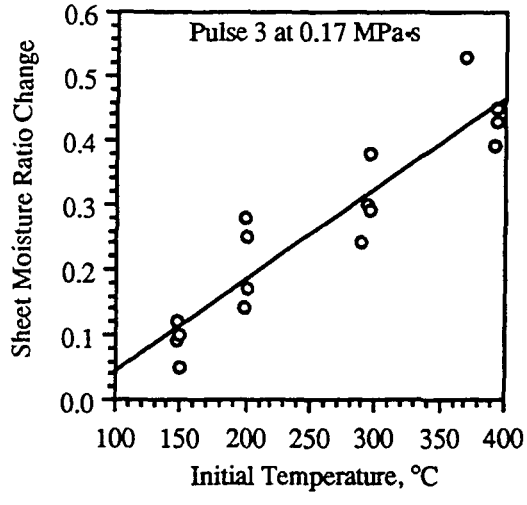

Figure B7. Moisture ratio change for the HKSP furnish with pulse shape 3 at 0.17 MPa·s.

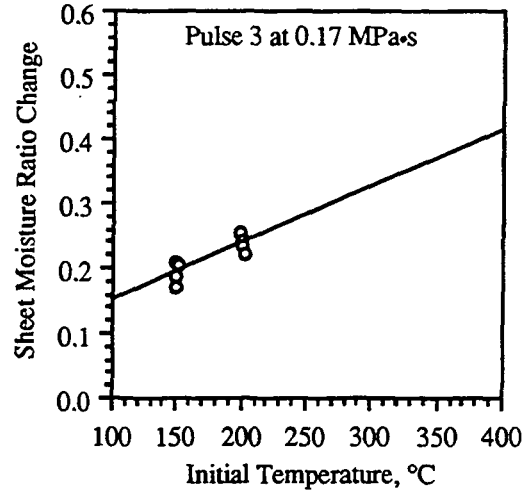

Figure B8. Moisture ratio change for the OCC furnish with pulse shape 3 at 0.17 MPa·s.

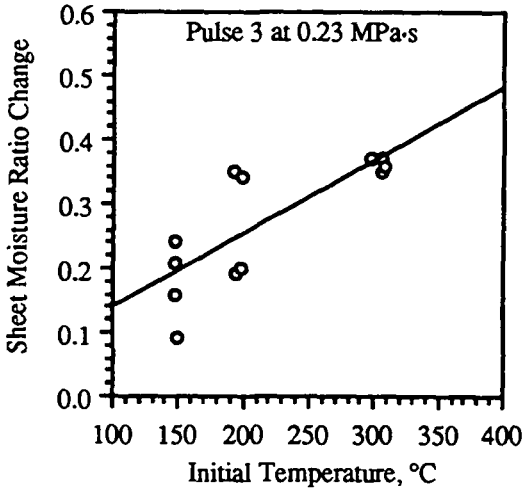

Figure B9. Moisture ratio change for the HKSP furnish with pulse shape 3 at 0.23 MPa·s.

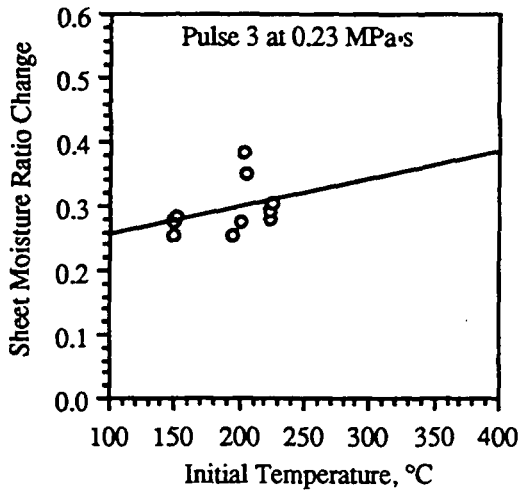

Figure B10. Moisture ratio change for the OCC furnish with pulse shape 3 at 0.23 MPa·s.

Figures B11-B20 show the outgoing solids for each impulse drying case. Data for delaminated samples are not shown.

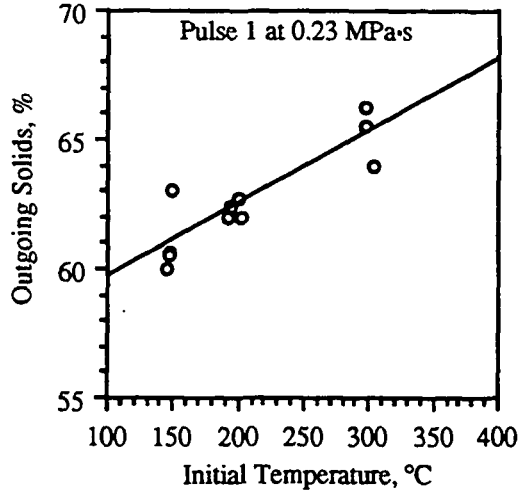

Figure B11. Outgoing solids for the HKSP furnish with pulse shape 1 at 0.23 MPa·s.

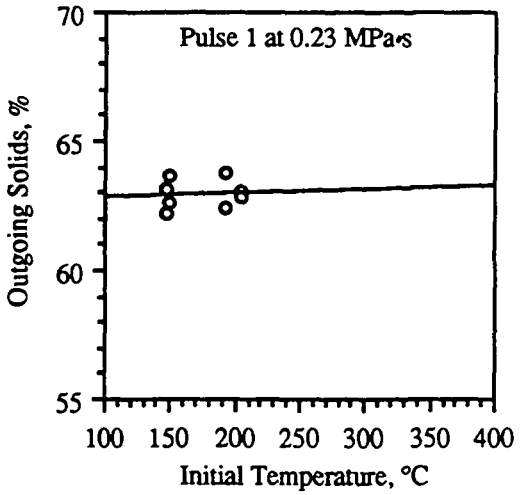

Figure B12. Outgoing solids for the OCC furnish with pulse shape 1 at 0.23 MPa·s.

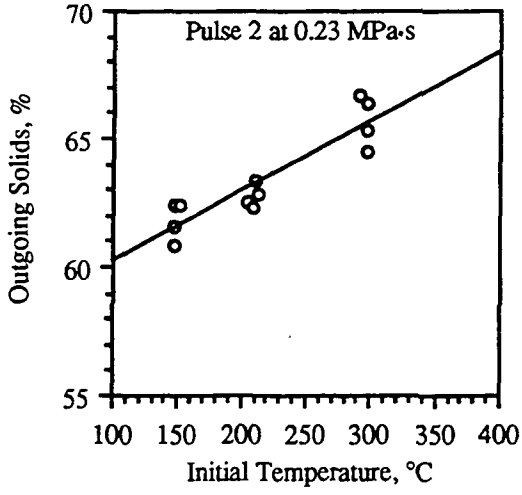

Figure B13. Outgoing solids for the HKSP furnish with pulse shape 2 at 0.23 MPa·s.

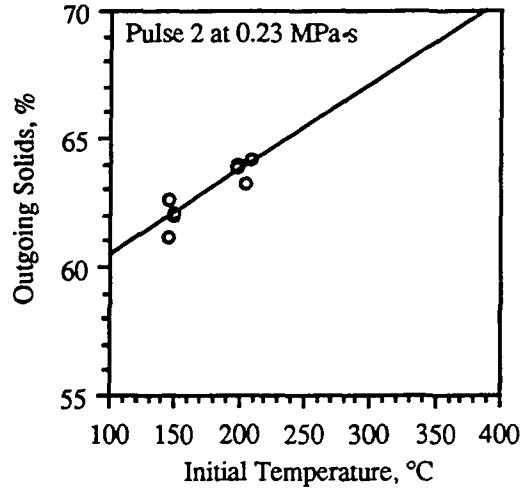

Figure B14. Outgoing solids for the OCC furnish with pulse shape 2 at 0.23 MPa·s.

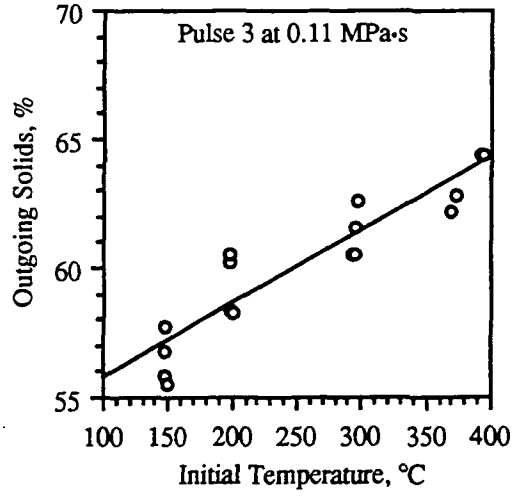

Figure B15. Outgoing solids for the HKSP furnish with pulse shape 3 at 0.11 MPa·s.

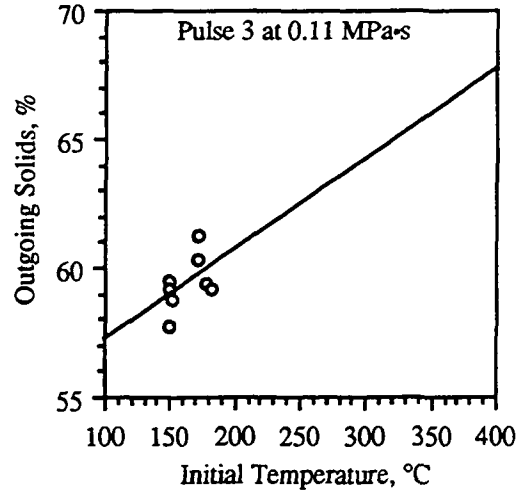

Figure B16. Outgoing solids for the OCC furnish with pulse shape 3 at 0.11 MPa·s.

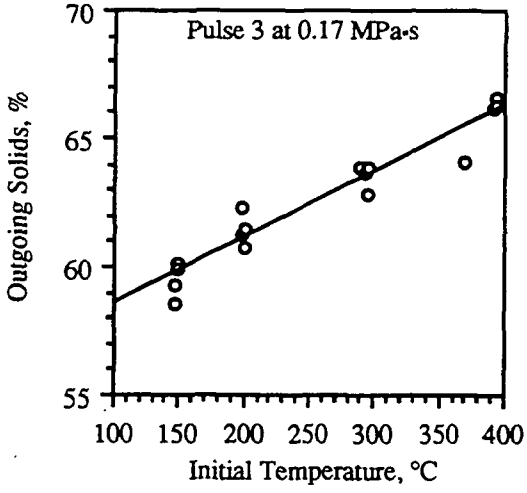

Figure B17. Outgoing solids for the HKSP furnish with pulse shape 3 at 0.17 MPa·s.

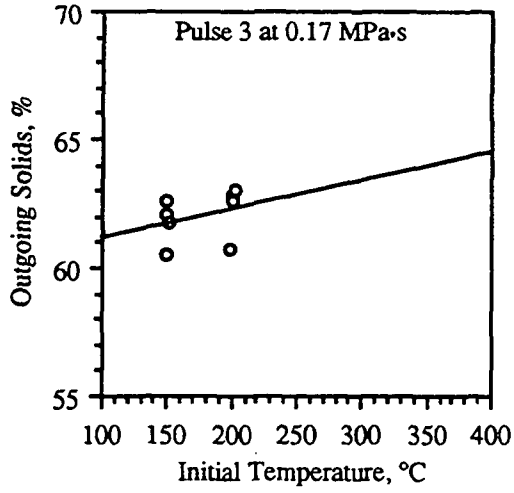

Figure B18. Outgoing solids for the OCC furnish with pulse shape 3 at 0.17 MPa·s.

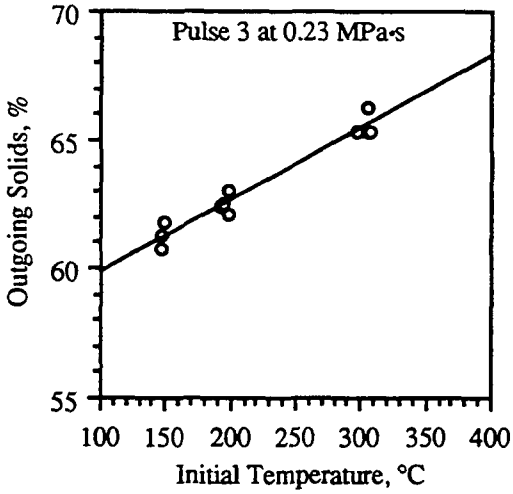

Figure B19. Outgoing solids for the HKSP furnish with pulse shape 3 at 0.23 MPa·s.

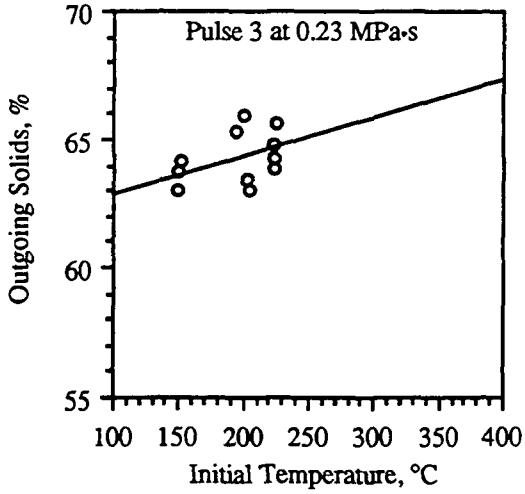

Figure B20. Outgoing solids for the OCC furnish with pulse shape 3 at 0.23 MPa·s.

Figures B21-B30 show the IPC density for each impulse drying case. Data for delaminated samples is not shown.

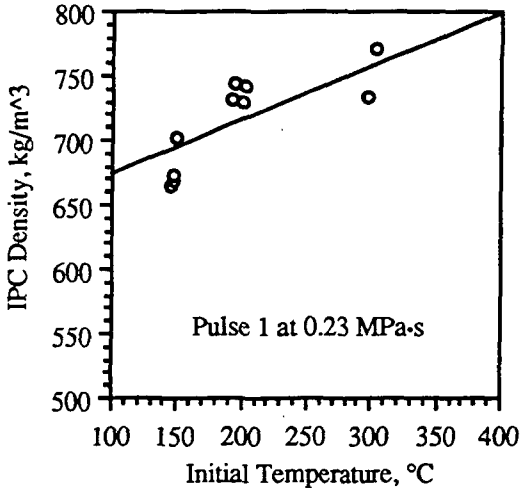

Figure B21. IPC density for the HKSP furnish with pulse shape 1 at 0.23 MPa·s.

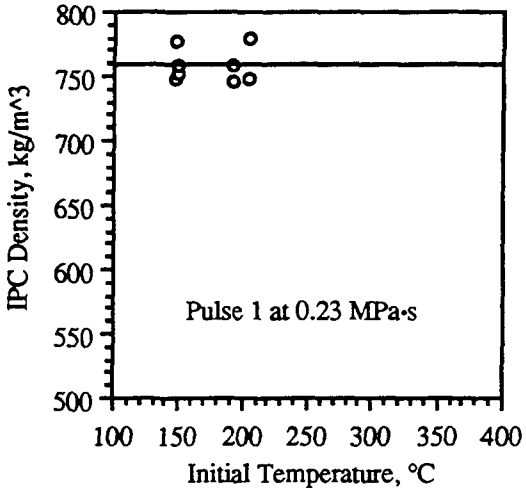

Figure B22. IPC density for the OCC furnish with pulse shape 1 at 0.23 MPa·s.

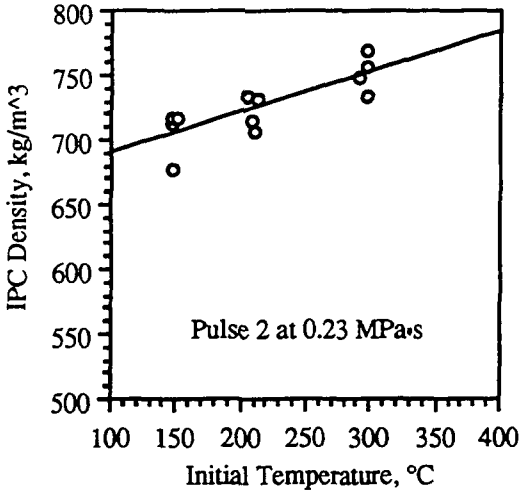

Figure B23. IPC density for the HKSP furnish with pulse shape 2 at 0.23 MPa·s.

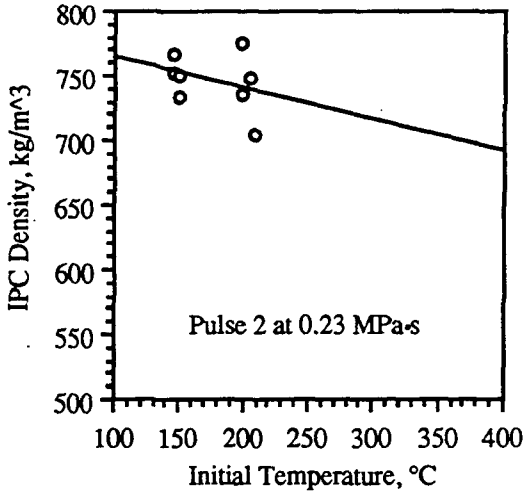

Figure B24. IPC density for the OCC furnish with pulse shape 2 at 0.23 MPa·s.

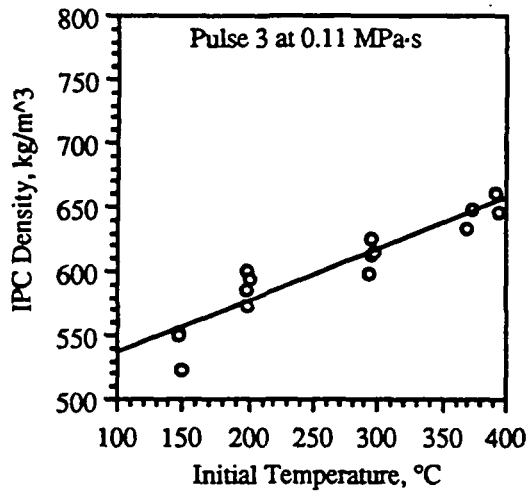

Figure B25. IPC density for the HKSP furnish with pulse shape 3 at 0.11 MPa·s.

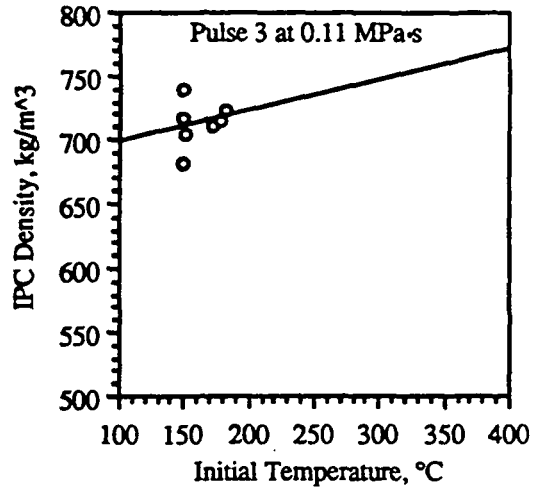

Figure B26. IPC density for the OCC furnish with pulse shape 3 at 0.11 MPa·s.

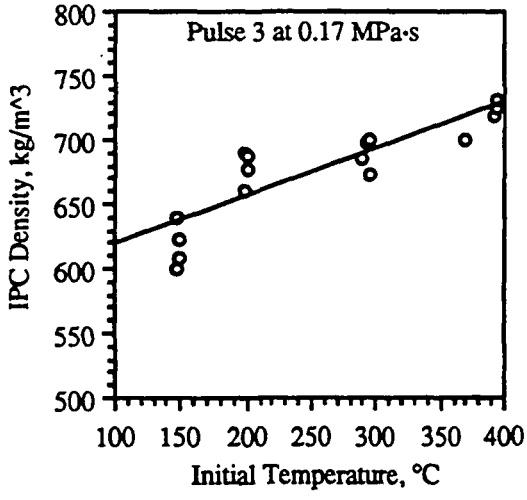

Figure B27. IPC density for the HKSP furnish with pulse shape 3 at 0.17 MPa·s.

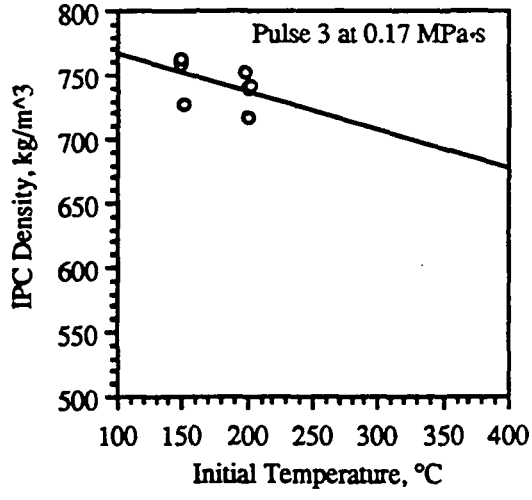

Figure B28. IPC density for the OCC furnish with pulse shape 3 at 0.17 MPa·s.

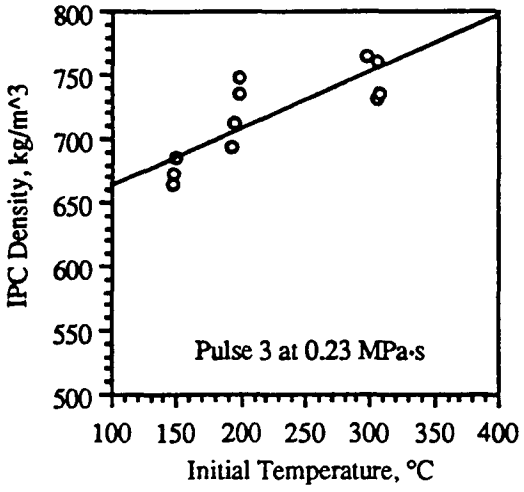

Figure B29. IPC density for the HKSP furnish with pulse shape 3 at 0.23 MPa·s.

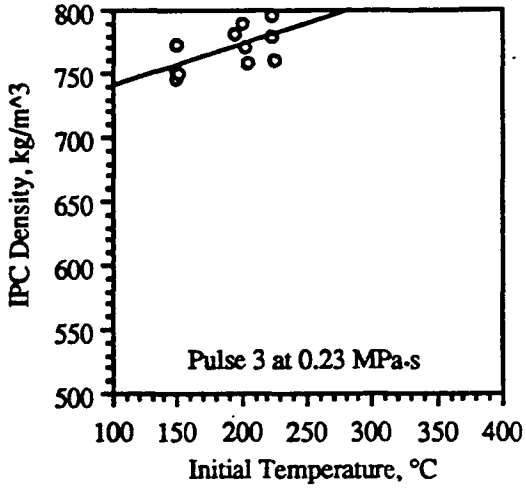

Figure B30. IPC density for the OCC furnish with pulse shape 3 at 0.23 MPa·s.

Figures B31-B40 show the STFI index for each impulse drying case. Data for delaminated samples are not shown.

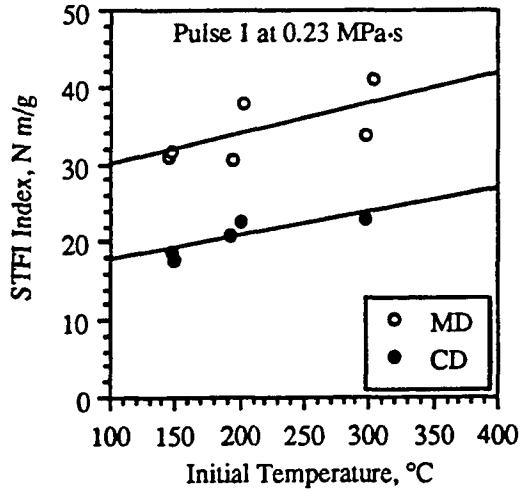

Figure B31. STFI index for the HKSP furnish with pulse shape 1 at 0.23 MPa·s.

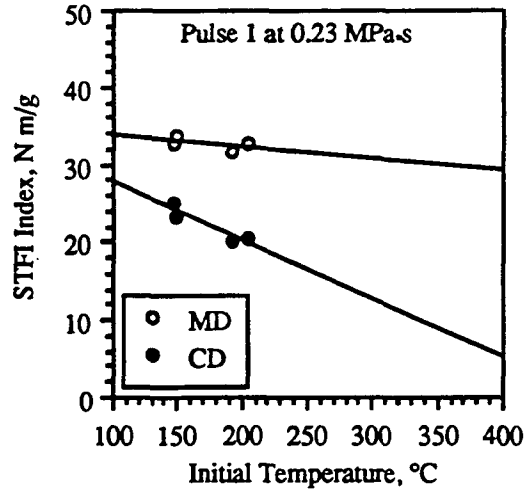

Figure B32. STFI index for the OCC furnish with pulse shape 1 at 0.23 MPa·s.

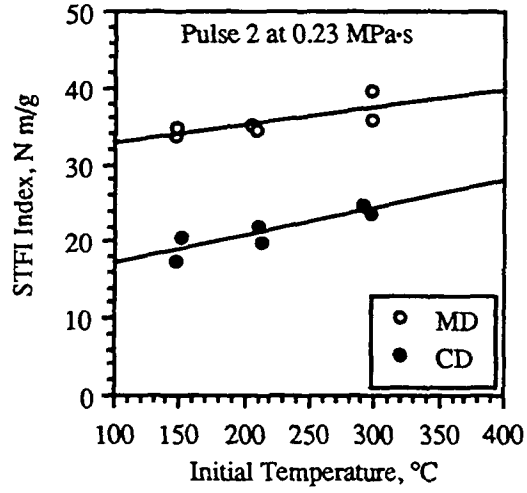

Figure B33. STFI index for the HKSP furnish with pulse shape 2 at 0.23 MPa·s.

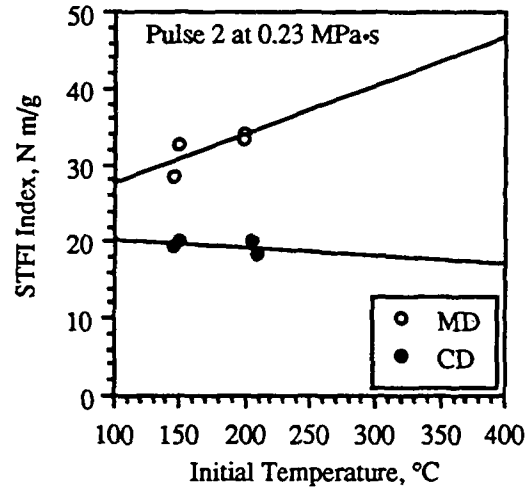

Figure B34. STFI index for the OCC furnish with pulse shape 2 at 0.23 MPa·s.

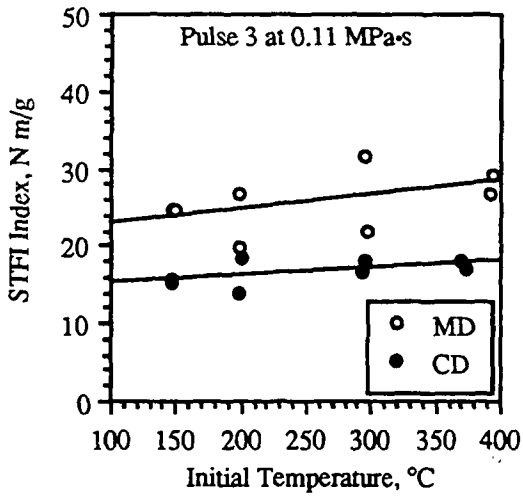

Figure B35. STFI index for the HKSP furnish with pulse shape 3 at 0.11 MPa·s.

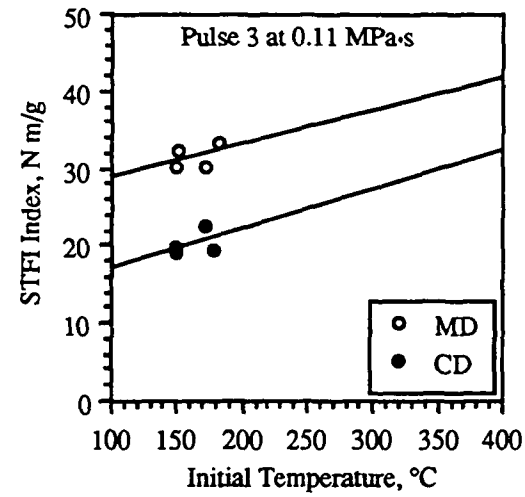

Figure B36. STFI index for the OCC furnish with pulse shape 3 at 0.11 MPa·s.

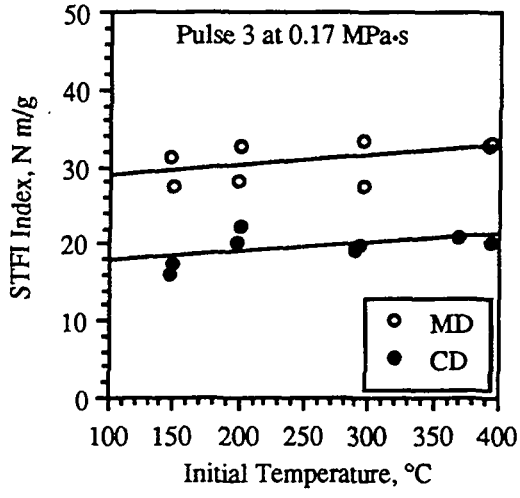

Figure B37. STFI index for the HKSP furnish with pulse shape 3 at 0.17 MPa·s.

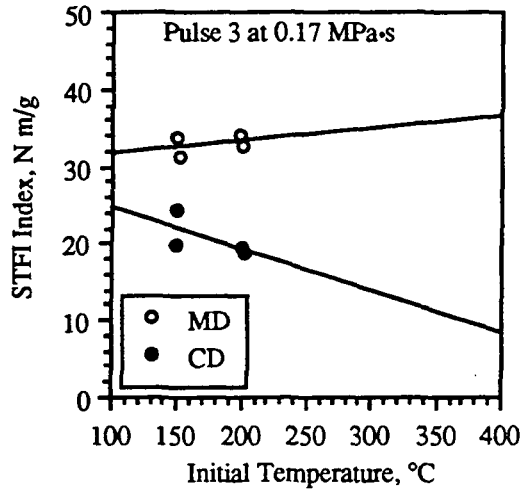

Figure B38. STFI index for the OCC furnish with pulse shape 3 at 0.17 MPa·s.

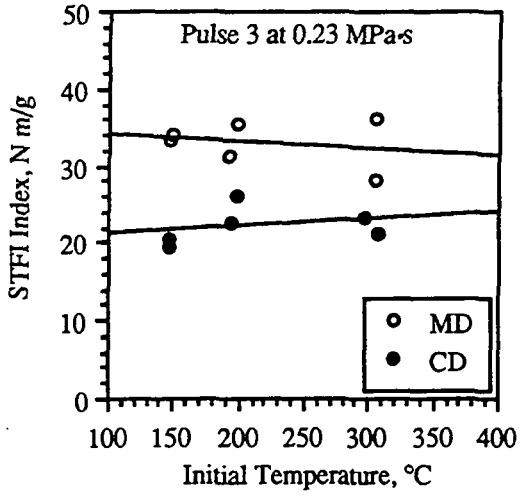

Figure B39. STFI index for the HKSP furnish with pulse shape 3 at 0.23 MPa·s.

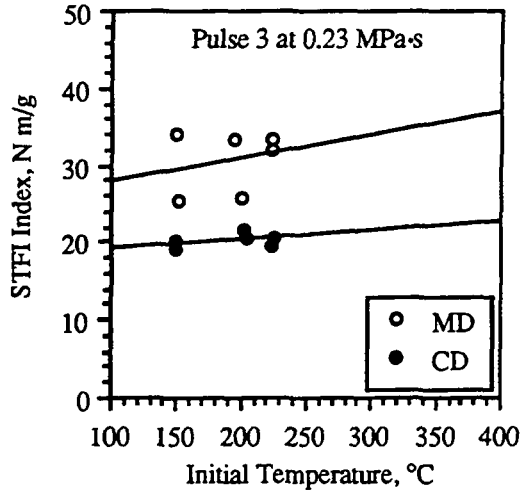

Figure B40. STFI index for the OCC furnish with pulse shape 3 at 0.23 MPa·s.